

Bis(imino)pyridines incorporating doubly fused 8-membered rings as conformationally flexible supports for cobalt ethylene polymerization catalysts

Zheng Wang,^{†,‡} Gregory A. Solan,^{†,#,*} Qaiser Mahmood,^{†,‡} Qingbin Liu,^{§,*} Yanping Ma,[†] Xiang Hao,[†] and Wen-Hua Sun^{†,‡,*}

[†]Key Laboratory of Engineering Plastics and Beijing National Laboratory for Molecular Science, Institute of Chemistry, Chinese Academy of Sciences, Beijing 100190, China.

[‡]CAS Research/Education Center for Excellence in Molecular Sciences, University of Chinese Academy of Sciences, Beijing 100049, China.

[#]Department of Chemistry, University of Leicester, University Road, Leicester LE1 7RH, UK.

[§]College of Chemistry and Material Science, Hebei Normal University, Shijiazhuang 050024, China.

ABSTRACT: Five distinct α,α' -bis(arylimino)-2,3:5,6-bis(hexamethylene)pyridine-cobalt(II) chloride complexes, $[2,3:5,6-\{C_5H_{10}C(NAr)\}_2C_5HN]CoCl_2$ (Ar = 2,6-Me₂C₆H₃ **Co1**, 2,6-Et₂C₆H₃ **Co2**, 2,6-*i*-Pr₂C₆H₃ **Co3**, 2,4,6-Me₃C₆H₂ **Co4**, 2,6-Et₂-4-MeC₆H₂ **Co5**), have been synthesized by the one-pot template reaction of α,α' -dioxo-2,3:5,6-bis(hexamethylene)pyridine with the corresponding aniline and cobalt(II) chloride in acetic acid. The molecular structures of **Co2** and **Co3** reveal distorted square pyramidal geometries with two conformationally flexible

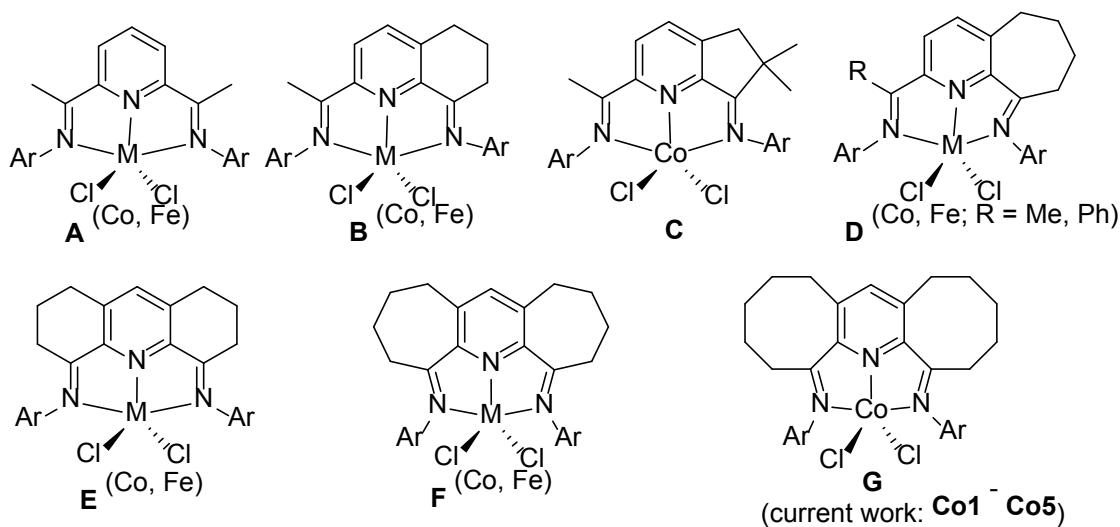
eight-membered rings a feature of the ligand manifold. On activation with either methylaluminoxane (MAO) or modified MAO (MMAO), all five complexes displayed high catalytic activities for ethylene polymerization (up to 3.62×10^6 g PE mol⁻¹ (Co) h⁻¹) generating strictly linear polyethylenes with the activity decreasing in the order: **Co4** > **Co5** > **Co1** > **Co2** > **Co3** (MAO) and **Co1** > **Co4** > **Co2** > **Co5** > **Co3** (MMAO). Moreover, the nature of the aluminoxane co-catalyst employed had a marked effect on the molecular weight and distribution (M_w/M_n) of the polymeric material obtained. For example using MAO, high molecular weight polyethylene ($M_w \approx 10^5$ g mol⁻¹) with a narrow monomodal molecular weight distribution (2.1 – 3.6) was a characteristic, while using MMAO, the polyethylene was of lower molecular weight ($M_w \approx 10^4$ g mol⁻¹) and exhibited a mono- to bimodal distribution (10.1 – 23.8) depending on the ratio of MMAO employed, temperature and run time.

INTRODUCTION

With the disclosure of highly active bis(imino)pyridine-cobalt and -iron catalysts for ethylene oligo-/polymerization towards the end of the 1990's (A in Chart 1),¹ the search for more potent and thermally stable systems has continued apace during the intervening years.^{2,3,4} In the main this search has been concerned with changes to the N-aryl groups^{3,4} of the tridentate NNN-ligand as well as to the substituents located on the imine-carbon atom.^{3f} Elsewhere altogether different NNN-ligand frames, such as 2-benzimidazolyl-6-iminopyridines,⁵ *N*-[(pyridin-2-yl)methylene]-8-aminoquinolines,⁶

2,8-bis(imino)quinolones⁷ and 2-imino-1,10-phenanthrolines,⁸ have emerged as compatible supports for cobalt and iron catalysts.^{2a,2h} Indeed, a 2-imino-1,10-phenanthroline-iron catalyst⁹ has been employed in a 500-ton scale pilot process for ethylene oligomerization.^{2h}

Chart 1 Bis(imino)pyridine-containing **A** and its fused derivatives **B – G**



As a more recent development, our group and others have been attracted by introducing controlled amounts of strain to the parent bis(imino)pyridine framework with a view to modifying the donor properties of the tridentate ligand and in-turn the performance of the catalyst.^{2a,2g-k} To realize this goal, the incorporation of fused carbocyclic rings to the central pyridine has been systematically implemented leading to pre-catalysts containing both singly and doubly fused derivatives with ring sizes of between five and seven (**B – F**, Chart 1).¹⁰⁻¹⁴ With particular regard to cobalt pre-catalysts,

use of **B**, containing a singly-fused six-membered ring (Chart 1),¹⁰ results in much higher activities and better thermal stability than the prototypical **A** and produces solely polyethylenes.^{10b} On the other hand, using **C** (Chart 1),¹¹ possessing a smaller five-membered ring, much lower activities are displayed.^{12a} However, the seven-membered ring system **D** (Chart 1),¹² exhibits the highest activity of this singly-fused series, the longest catalyst lifetime and best thermal stability.^{12b-c} With respect to the doubly-fused cobalt systems **E** and **F** (Chart 1), **E** shows high activity but affords a less desirable mixture of polyethylenes and oligomers.¹³ By contrast, the seven-membered ring analog **F**, proved highly efficient and affords strictly linear vinyl-polyethylenes.^{14a-b} Notably, such polymers are in demand and indispensable in the production of long-chain branched copolymers, functional polymers as well as coating materials.^{14b,15}

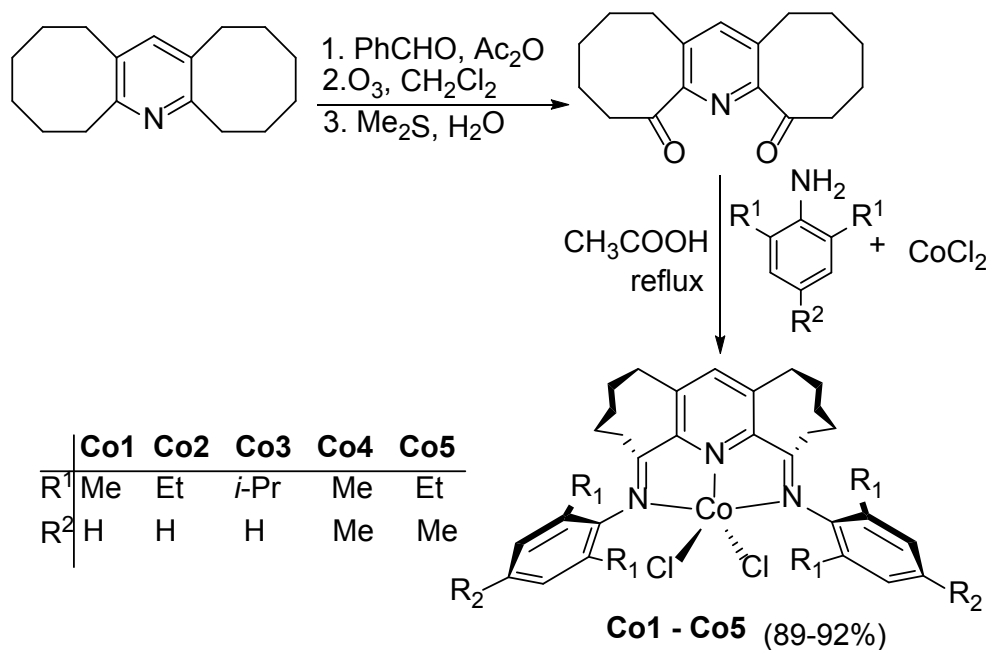
In this program, we target a new series of divalent cobalt chloride complexes bearing chelating α,α' -bis(arylimino)-2,3:5,6-bis(hexamethylene)pyridines (**G**, Chart 1), in which the central pyridine is fused by two non-rigid eight-membered rings and their α -positions linked to a range of electronically and sterically different N-aryl groups. An in-depth study is conducted to optimize catalytic performance of these pre-catalysts in ethylene polymerization using two different activators and to examine how these structural and co-catalyst variations impact on catalytic activity and polymer product. In addition to polymer characterization, full synthetic procedures and characterization data for the complexes are reported.

RESULTS AND DISCUSSION

Synthesis and Characterization of Co1 – Co5

The α,α' -bis(arylimino)-2,3:5,6-bis(hexamethylene)pyridine-cobalt(II) chlorides, $[2,3:5,6-\{C_5H_{10}C(NAr)\}_2C_5HN]CoCl_2$ (Ar = 2,6-Me₂C₆H₃ **Co1**, 2,6-Et₂C₆H₃ **Co2**, 2,6-*i*-Pr₂C₆H₃ **Co3**, 2,4,6-Me₃C₆H₂ **Co4**, 2,6-Et₂-4-MeC₆H₂ **Co5**), have been prepared in reasonable yield by the one-pot template reactions of α,α' -dioxo-2,3:5,6-bis(hexamethylene)pyridine,¹⁶ the corresponding aniline and CoCl₂·4H₂O in acetic acid at reflux for 12 hours (Scheme 1). The free ligands themselves have not proved amenable to isolation as has been observed with related doubly-fused bis(imino)pyridines, an observation that is likely attributable to decomposition via pathways involving imine–enamine tautomerization.^{13,14} The precursor diketone, α,α' -dioxo-2,3:5,6-bis(hexamethylene)pyridine,¹⁶ is not commercially available and can be prepared in two steps by firstly the condensation reaction of 2,3:5,6-bis(hexamethylene)pyridine^{16a} with benzaldehyde and then oxidation of the intermediate by ozone in dichloromethane at -40 °C using previously reported procedures (Scheme 1); the ¹H/¹³C NMR spectra of both 2,3:5,6-bis(hexamethylene)pyridine α,α' -dioxo-2,3:5,6-bis(hexamethylene)pyridine are consistent with that reported in literature.^{16a} All the cobalt complexes have been characterized by ¹H NMR, FT-IR spectroscopy, magnetic measurements and elemental analysis. In addition, **Co2** and **Co3** have been the subject of single crystal X-ray diffraction studies.

Scheme 1 Synthetic route to **Co1 - Co5** from 2,3:5,6-bis(hexamethylene)pyridine



Single crystals of **Co2** and **Co3** suitable for the X-ray determinations were grown by slow diffusion of diethyl ether into a dichloromethane solution of the corresponding complex. The molecular structures of **Co2** and **Co3** are shown in Figs. 1 and 2; selected bond lengths and angles are collected in Table 1. The structures are similar and will be discussed together. Both consist of a single cobalt center surrounded by three nitrogen atoms belonging to the α,α' -bis(arylimino)-2,3:5,6-bis(hexamethylene)pyridine and two chloride ligands to complete a five-coordinate geometry. The structures differ in the nature of the aryl groups linked to the exterior nitrogen donors; 2,6-diethylphenyl for **Co2** and 2,6-diisopropylphenyl for **Co3**. The five-coordinate geometries can be best described as distorted square-pyramidal with the three nitrogen atoms and one chloride atom (Cl2) forming the basal plane and Cl1 filling the apical position. The cobalt atom sits at a

distance of 0.483 Å above the basal plane for **Co2** and 0.526 Å for **Co3** in a manner similar to that observed in related NNNCoCl₂ species.^{1,12b,12c,13,14a} The central Co–N_{pyridine} bond length [2.0720(18) (**Co2**) 2.0790(2) (**Co3**) Å] is shorter than the exterior Co–N_{imino} ones [2.1180(18) – 2.1633(18) Å], while the N2–Co1–N1 [74.62(10)° (**Co2**), 74.04(7)° (**Co3**)] and N(1)–Co(1)–N(3) [138.33(10)° (**Co2**), 141.70(7)° (**Co3**)] angles within each five-membered chelate ring are consistent with previous observations.^{10,11a,12b-c,13,14a} The torsion angles for N(1)–C(1)–C(8)–N(2) [7.20° (**Co2**), 8.90° (**Co3**)] and N(3)–C(17)–C(11)–N(2) [-5.21° (**Co2**), -15.06° (**Co3**)] highlight the deviation from co-planarity between the pyridine ring and the neighboring imine vectors. Notably, these deviations are generally larger than that observed for the corresponding torsion angles in the smaller seven-membered ring analog **F** (av. = 6.6(4)° and -6.0(4)°).^{14a} Furthermore, the Co–N_{pyridine} bond length [2.0790(2) Å (**Co2**), 2.0720(18) Å (**Co3**)] is longer than that observed in **A** (2.051(3) Å),^{1c} **B** (2.040(3) Å),^{10b} **D** (2.036(4)-2.052(5) Å)^{12b,c} and **E** (2.037(4) Å),¹³ but close to that found in **F** (2.082(3) Å).^{14a} By contrast, the Co–N_{imine} bonds [2.1180(18) - 2.1633(18) Å] are shorter than found in **A**,^{1c} **B**,^{10b} **D**^{12b,c} and **E** (range: 2.193–2.320 Å, Chart 1),¹³ but similar to those observed in **F** [2.128(3) and 2.176(3) Å].^{14a} Clearly, the presence of the two fused eight-membered rings in **Co2** and **Co3** is causing some structural reorganization of the tridentate ligand. Within the saturated section of the eight membered rings (C2-C3-C4-C5-C6 and C12-C13-C14-C15-C16) the expected non-planar puckered arrangement is adopted. The N-aryl rings are almost perpendicular to the coordination plane with dihedral angles of 85.85° and 89.84° for

Co2 and 87.73° and 88.85° for **Co3**, respectively. There are no intermolecular contacts of note.

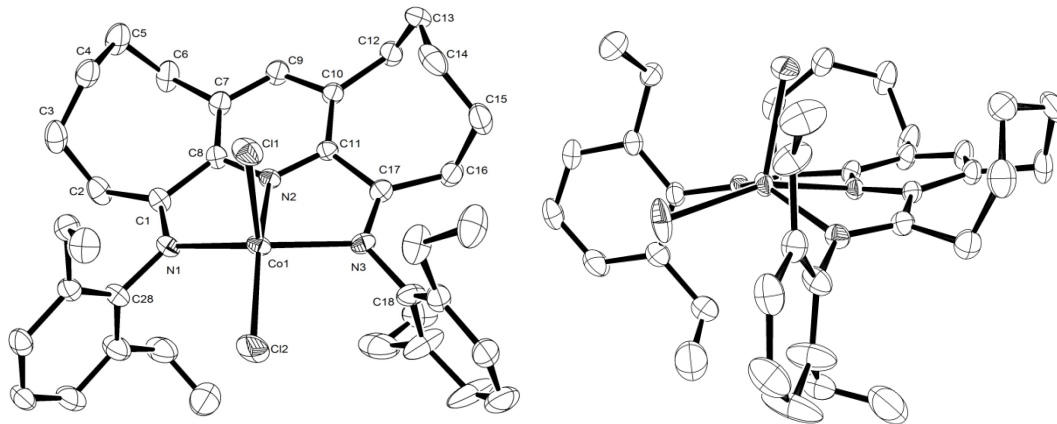


Fig. 1. ORTEP representations of **Co2**. Thermal ellipsoids are shown at 30% probability and hydrogen atoms have been omitted for clarity.

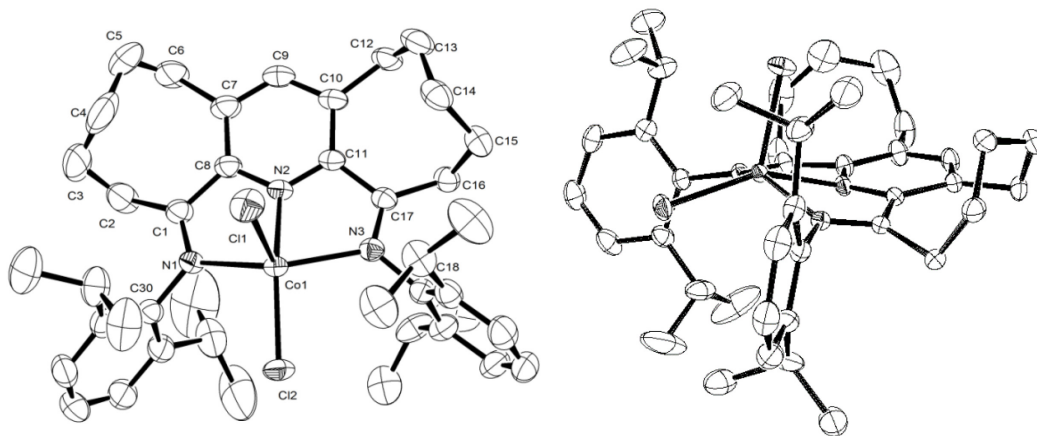


Fig. 2. ORTEP representations of **Co3**. Thermal ellipsoids are shown at 30% probability and hydrogen atoms have been omitted for clarity.

Table 1 Selected bond lengths and angles for **Co2** and **Co3**

	Co2	Co3
Bond lengths (Å)		
Co(1)–N(1)	2.1180(3)	2.1633(18)
Co(1)–N(2)	2.0790(2)	2.0720(18)
Co(1)–N(3)	2.1370(3)	2.1469(18)
Co(1)–Cl(1)	2.2995(10)	2.3007(8)
Co(1)–Cl(2)	2.2389(10)	2.2503(7)
Bond angles (°)		
N(1)–Co(1)–N(2)	74.62(10)	74.04(7)
N(1)–Co(1)–N(3)	138.33(10)	141.70(7)
N(2)–Co(1)–N(3)	73.91(10)	75.41(7)
N(1)–Co(1)–Cl(2)	100.43(8)	97.74(5)
N(2)–Co(1)–Cl(2)	159.54(8)	89.97(6)
N(3)–Co(1)–Cl(2)	99.57(8)	98.99(5)
N(1)–Co(1)–Cl(1)	103.59(8)	98.26(5)
N(2)–Co(1)–Cl(1)	88.42(7)	152.85(6)
N(3)–Co(1)–Cl(1)	102.14(8)	104.27(5)
Cl(2)–Co(1)–Cl(1)	112.01(5)	117.02(4)

The IR spectra of **Co1** – **Co5** displayed strong absorption bands around 1596 cm⁻¹ consistent with the coordination of both imine nitrogen atoms.¹⁰⁻¹⁴ Furthermore, the microanalytical data for the complexes were in full agreement with elemental compositions of general formula LCoCl₂. Characteristically broad paramagnetically shifted peaks are a feature of the ¹H NMR spectra of all the complexes [recorded in

deuterated chloroform (CDCl₃) at ambient temperature]. The assignment of the peaks in **Co1** - **Co5** has been made through a comparison with data recorded for related Co(II) complexes, relative integration and proximity to the paramagnetic center.^{1c,3a,3b} For all five complexes, a distinct downfield peak for the *para*-pyridyl proton at δ 41.92_{av.} (see Figures S5-S9) is visible, while the *meta*-aryl protons can be seen more upfield at δ 13.64_{av.} (see Figures S5-S9 for **Co1** - **Co5**). By contrast, the ketimine protons (N=CCH₂) can be seen at δ 15.09_{av.} and the methyl protons (Ar-Me or CHMe₂) as a broad and upfield peak at δ -14.76_{av.}. In addition, multiple peaks for the cycloalkyl protons (CH₂) are evident between δ 3.78 – δ 0.83. Moreover, all five cobalt complexes display magnetic moments of $\sim 4.1 \mu_B$, consistent with three unpaired electrons (Evans NMR method^{1b,3a,3b,17}).

Catalyst evaluation for ethylene polymerization

In previously reported studies,^{1,2,4} cobalt(II) chloride complexes of the type **A** – **F** (Chart 1) have been shown to exhibit their optimal catalytic performance in the presence of either methyl aluminoxane (MAO) or modified MAO (MMAO) as co-catalyst.^{1,10-14} Hence, this investigation focuses on these two co-catalysts using mesityl-containing **Co4** as the test pre-catalyst. Optimizations of the Al/Co ratio, reaction temperature and catalyst lifetime were performed independently using **Co4**/MAO and **Co4**/MMAO before the remaining pre-catalysts, **Co1** – **Co3**, **Co5**, were evaluated with each co-catalyst. All polymeric materials were characterized by gel permeation chromatography (GPC) and differential scanning calorimetry (DSC), while the microstructural properties of selected samples were examined using high-temperature ¹³C NMR spectroscopy. In all cases, gas

chromatography was used to detect the presence of any oligomeric products.

Using Co1 – Co5/MAO. In the first instance, the effect of the molar ratio of Al/Co on the catalytic performance of Co4/MAO was explored. Typically the runs were performed in toluene under 10 atmospheres of ethylene pressure over 30 minutes with the ratio varied between 1000 – 3000 (entries 1 – 7, Table 2). The optimum activity was observed as 2.89×10^6 g (PE) mol⁻¹ (Co) h⁻¹ with a molar ratio of 1500 (entry 3, Table 2). The molecular weight (M_w) of the polymer was found to decrease by more than half from

Table 2. Ethylene polymerization results using Co1 – Co5/MAO^a

Entry	Pre-cat.	Al/Co	T (°C)	t (min)	Yield (g)	Act. ^b	M_w^c	M_w/M_n^c	T_m^d (°C)
1	Co4	1000	30	30	3.75	2.50	540.1	2.6	135.5
2	Co4	1250	30	30	3.86	2.57	497.9	2.2	135.1
3	Co4	1500	30	30	4.33	2.89	422.7	2.7	135.0
4	Co4	1750	30	30	3.85	2.57	380.0	2.4	135.3
5	Co4	2000	30	30	3.78	2.52	346.1	2.5	135.3
6	Co4	2500	30	30	3.35	2.23	336.3	2.2	135.2
7	Co4	3000	30	30	3.13	2.08	250.1	3.0	135.2
8	Co4	1500	20	30	2.12	1.41	463.7	2.9	135.7
9	Co4	1500	40	30	2.90	1.93	251.2	4.4	135.5
10	Co4	1500	50	30	2.63	1.75	182.9	3.6	135.5
11	Co4	1500	60	30	2.39	1.60	109.1	2.9	135.6
12	Co4	1500	70	30	2.12	1.41	84.1	3.3	135.6
13	Co4	1500	30	15	2.56	3.14	269.2	2.7	135.8
14	Co4	1500	30	45	4.56	2.03	401.9	2.9	136.4

15	Co4	1500	30	60	5.00	1.67	500.2	3.7	136.0
16 ^e	Co4	1500	30	30	0.88	0.59	264.9	2.8	136.5
17 ^f	Co4	1500	30	30	trace	--	--	--	--
18	Co1	1500	30	30	3.63	2.42	405.3	2.7	136.7
19	Co2	1500	30	30	2.48	1.65	379.4	3.5	135.9
20	Co3	1500	30	30	0.85	0.57	539.1	2.6	134.3
21	Co5	1500	30	30	4.08	2.72	432.7	3.2	135.6

^a Conditions: 3.0 μmol of **Co4**; 100 mL toluene, 10 atm ethylene. ^b Values in units of 10^6 g(PE) mol^{-1} (Co) h^{-1} . ^c Determined by GPC, and M_w : kg mol^{-1} . ^d Determined by DSC. ^e 5 atm ethylene. ^f 1 atm ethylene.

540.1 to 250.1 kg mol^{-1} on changing the ratio from 1000 to 3000 which can be ascribed to increased chain transfer from cobalt to aluminum on increasing the amount of alkyl aluminum reagent.^{1c,14,18} On the other hand, the molecular weight distribution remained narrow ($M_w/M_n = 2.2$ to 3.0) across the range of Al/Co ratios; their GPC curves further illustrate this behavior (Fig. 3).

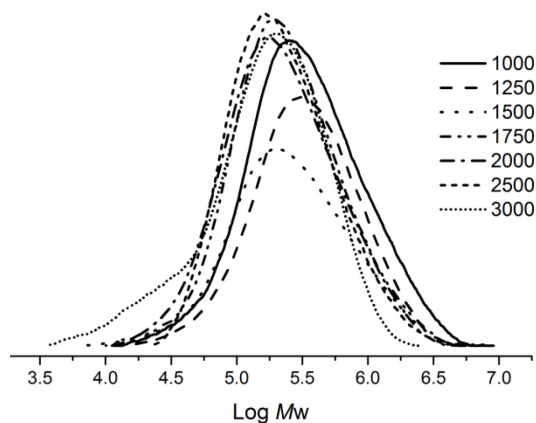


Fig. 3 GPC curves for the polyethylenes obtained using **Co4**/MAO with various Al/Co ratios (10 atm of ethylene, 30 °C and 30 minute run time)

Secondly, the influence of temperature on the polymerization using **Co4**/MAO was

investigated with the Al/Co molar ratio set at 1500 (entries 3 and 8 – 12, Table 2). On raising the temperature from 20 to 70 °C, a peak in activity at 2.89×10^6 g PE mol⁻¹(Co) h⁻¹ was observed at 30 °C (entry 3, Table 2). Above 30 °C the activity steadily drops reaching a minimum at 70 °C of 1.41×10^6 g PE mol⁻¹(Co) h⁻¹. Inspection of the GPC curves, shown in Fig. 4, illustrates how the M_w steadily declines from 463.7 to 84.1 kg mol⁻¹ as the temperature is raised from 20 to 70 °C, an observation that can be accredited to either increased chain transfer to aluminum or chain termination by β -H elimination at the higher temperatures.^{1c,8f,12c,12d} Meanwhile, the molecular weight distribution remained relatively narrow (2.9 – 4.4) over the temperature range consistent with an active species displaying single-site behavior.

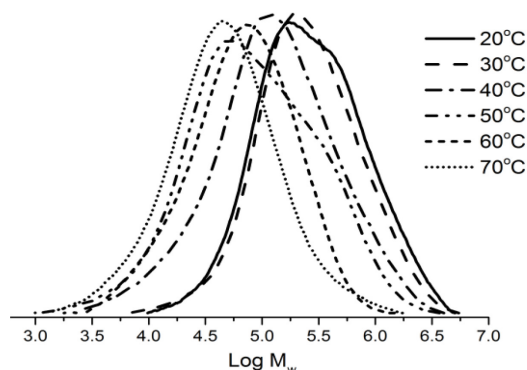


Fig. 4. GPC curves for the polyethylenes obtained using **Co4**/MAO at different reaction temperatures (10 atm of ethylene, Al/Co ratio = 1500 and 30 minute run time)

Thirdly, the lifetime of the **Co4**/MAO catalyst was probed by conducting the polymerization over 15, 30, 45 and 60 minute run times (entries 3 and 13–15, Table 2). The highest activity (3.14×10^6 g PE mol⁻¹(Co) h⁻¹) was achieved after 15 minutes which can be attributed to the active species being rapidly formed after the addition of MAO

and then gradually deactivating (entry 13, Table 2).^{14a,19} Nevertheless, there were sufficient active species over the longer run times leading to longer chains and in-turn a gradual increase in the molecular weight of the resultant polymeric material (Fig. 5). A modest increase in the molecular weight distribution (from 2.1 to 3.7) was also observed over more extended run times. On lowering the ethylene pressure from 10 to 5 atmospheres a dramatic drop in catalytic activity was evident (entries 16 vs. 3, Table 2), while under 1 atmosphere of ethylene only trace amounts of polymer were detectable (entry 17, Table 2).

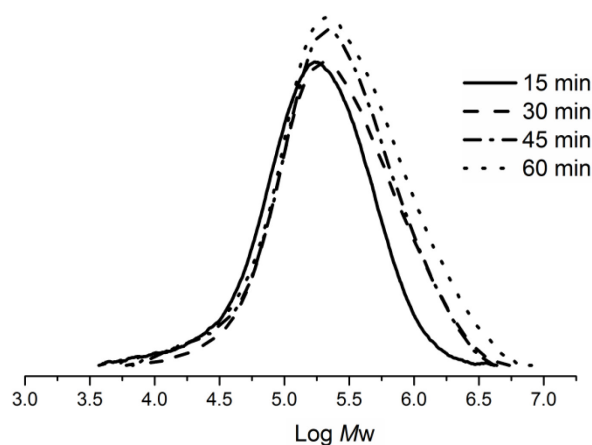


Fig. 5. GPC curves for the polyethylenes obtained using **Co4**/MAO at different run times (10 atm of ethylene, Al/Co ratio = 1500 and at 30 °C)

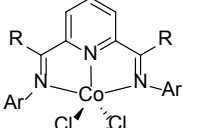
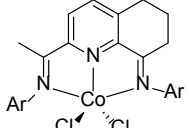
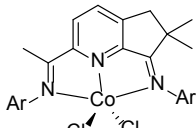
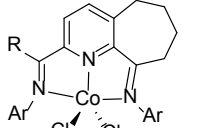
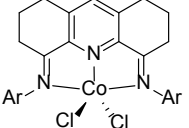
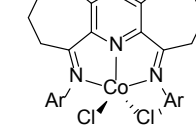
Finally, the remaining four pre-catalysts, **Co1** – **Co3** and **Co5**, were screened for ethylene polymerization employing the optimized conditions established for **Co4**/MAO (*viz.*, Al/Co = 1500, run temperature = 30 °C). Collectively, all the cobalt catalysts exhibited high activities (range: $0.57 - 2.89 \times 10^6$ g PE mol⁻¹(Co) h⁻¹; entries 3, 18 – 21, Table 2) and were found to decrease in the order: **Co4** (2,4,6-trimethyl) > **Co5** (2,6-diethyl-4-methyl) > **Co1** (2,6-dimethyl) > **Co2** (2,6-diethyl) > **Co3** (2,6-diisopropyl). Clearly both steric and electronic effects imparted by the ligand influence catalytic

performance.^{1,10b,14a,20} With regard to steric properties, an increase in the steric bulk of the ligands leads to a reduction in the activity with the most hindered system **Co3** showing the lowest activity of the series. On other hand **Co3** gave the polymer with the highest molecular weight (539.1 kg mol⁻¹, entry 20 in Table 2), which highlights the role played by the bulky substituent in inhibiting chain transfer during the polymerization.^{1,4,10-14} Meanwhile, the observation that **Co4** (2,4,6-trimethyl) is more active than **Co1** (2,6-dimethyl) (entries 3 and 18, Table 2) and **Co5** (2,6-diethyl-4-methyl) more active than **Co2** (2,6-diethyl) (entries 19 and 20, Table 2) highlights the electronic effect played by the *para*-methyl group on catalytic activity; the improved solubility of these *para*-methyl species in the polymerization solvent is also a plausible contributing factor.^{3k,10,14a,b} Once again, all the polyethylenes obtained display characteristically narrow polydispersity (PDI = 2.6 – 3.5) and high melting temperatures (~135 °C) with sharp endotherm peaks in their DSC traces (see SI); the latter characteristic of highly linear materials. To support this conclusion, a sample of the polyethylene obtained using **Co4**/MAO (entry 3, Table 2) was characterized by ¹³C NMR spectroscopy (recorded in 1,1,2,2-[D₂] tetrachloroethane at 135 °C). The spectrum revealed one singlet peak around δ 30.00 (Fig. S5) assignable to the $-(CH_2)_n-$ repeat unit of a linear polyethylene.^{11b,13a,14c}

In comparison with previously reported cobalt pre-catalysts such as **A**, **B**, **D** and **E** (Chart 2),^{1,10b,12b-c,13} the current systems, **Co1** - **Co5**, under comparable polymerization conditions (namely MAO as co-catalyst and 10 atmospheres of ethylene pressure), exhibit relatively lower catalytic activity and indeed similar to that reported for the

doubly fused F-type pre-catalyst (Chart 2). On the other hand, the resulting polymers formed using **Co1** – **Co5**/MAO exhibit the highest molecular weight (range: 379.4 – 539.1 kg mol⁻¹) of the series. It is uncertain as to the origin of this variation but may be due to the reduced ring tension present within the two eight-membered rings in **Co1** – **Co5** causing the rate of chain transfer to decrease and hence encouraging chain growth.

Chart 2 Comparison of the M_w , PDI and activity of previously reported cobalt pre-catalysts (**A** – **F**) with MAO as activator under related conditions

 <p>A₁ (R = Me), A₂ (R = H)_{1c}</p>	 <p>B_{10b}</p>	 <p>C_{11a}</p>
<p>A₁ A₂</p> <p>Mw(g/mol) 2.57 x 10⁵ 1.60 x 10³</p> <p>PDI 144.5 2.6</p> <p>Activity 1.7 x 10⁷ 3.40 x 10⁶</p> <p>(gPE/mol(Co)/h)</p>	<p>Mw (g/mol) 910</p> <p>PDI 1.5</p> <p>Activity 1.09 x 10⁷</p> <p>(gPE/mol(Co)/h)</p>	<p>M_w (g/mol) 3.73 x 10⁵</p> <p>PDI 4.9</p> <p>Activity 2.89 x 10⁵</p> <p>(gPE/mol(Co)/h)</p>
 <p>D₁ (R = Me)_{1,12b} D₂ (R = Ph)_{12c}</p>	 <p>E₁₃</p>	 <p>F_{14a}</p>
<p>D₁ D₂</p> <p>Mw(g/mol) 3.20 x 10³ 4.64 x 10³</p> <p>PDI 1.8 2.2</p> <p>Activity 8.20 x 10⁶ 8.65 x 10⁶</p> <p>(gPE/mol(Co)/h)</p>	<p>Mw(g/mol) 930</p> <p>PDI 1.5</p> <p>Activity 2.54 x 10⁷</p> <p>(gPE/mol(Co)/h)</p>	<p>Mw(g/mol) 4.6 x 10³</p> <p>PDI 2.1</p> <p>Activity 3.69 x 10⁶</p> <p>(gPE/mol(Co)/h)</p>

Using Co1 – Co5/MMAO. To complement the study performed using MAO as co-catalyst, we also explored the activation of **Co1** – **Co5** using MMAO; the results are collected in Table 3. As before the optimization of the polymerization conditions was performed using **Co4** with the pressure of ethylene in the initial screen set at 10

atmospheres and the run temperature at 30 °C. On varying the Al/Co molar ratio from 1000 to 3000 (entries 1 – 7, Table 3), a maximum in catalytic activity was achieved of 1.58×10^6 g PE mol⁻¹(Co) h⁻¹ with the ratio at 1750. It was also evident that the molecular weight of the polymers decreased markedly from 120.7 to 48.4 kg mol⁻¹ as the Al/Co molar ratio was increased. A further striking feature was the variation in the molecular weight distribution (2.8 to 17.6) which became particularly broad when the Al/Co ratio was raised above 1500 (entries 1 – 7, Table 3). This broadening of the PDI represents quite different behavior to that observed with **Co4**/MAO but resembles that noted for **A**- and **B**-type iron pre-catalysts^{10a} and some bimetallic cobalt complexes.²⁰ Indeed, given the observation of two M_p peaks (peak 1 and peak 2) in their GPC curves (Fig. 6), the distribution becomes bimodal as the amount of co-catalyst is increased with the lower molecular weight fraction becoming more significant with larger amounts of MMAO (Fig. 6).

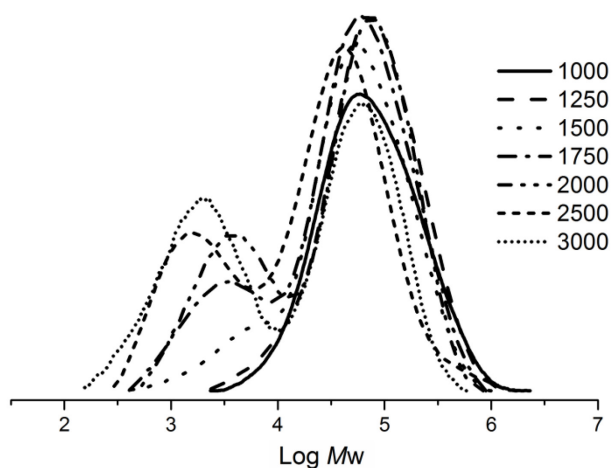


Fig. 6 GPC curves for the polyethylenes obtained using **Co4**/MMAO with various Al/Co ratios (10 atm of ethylene, 30 °C and 30 minute run time)

These results are consistent with chain transfer to aluminum playing an important role in the generation of the lower molecular weight fraction (*vide infra*).^{1c,10a} Surprisingly, the appearance of a lower molecular weight fraction with large amounts of MAO was not a feature in the earlier **Co4**/MAO runs (see Fig. 3). A plausible explanation for this difference in behavior may derive from higher amounts of AlMe₃ that are present in commercial samples of MMAO as compared to that in MAO. This higher concentration would then lead to an increase in the rate of chain transfer and in-turn a reduction in chain propagation.

Table 3 Ethylene polymerization results using **Co1 – Co5**/MMAO^a

Entry	Pre-cat	Al/Co	T (°C)	t (min)	Yield (g)	Act. ^b	M_p^c		M_w^c	M_w/M_n^c	T_m^d (°C)
							peak 1 %	peak 2 %			
1	Co4	1000	30	30	2.20	1.47	63.9 (100%)	-	120.7	2.8	134.9
2	Co4	1250	30	30	2.25	1.50	60.2 (100%)	-	119.6	2.8	134.6
3	Co4	1500	30	30	2.31	1.54	43.3 (100%)	-	86.4	4.9	134.4
4	Co4	1750	30	30	2.38	1.58	40.5 (95%)	2.4 (5%)	82.7	9.1	134.2
5	Co4	2000	30	30	2.06	1.37	36.2 (88%)	3.6 (11%)	77.8	9.4	133.9
6	Co4	2500	30	30	1.75	1.16	24.4 (78%)	5.1 (21%)	52.9	13.0	133.8
7	Co4	3000	30	30	1.70	1.13	21.3 (63%)	6.6 (37%)	48.4	17.6	133.5
8	Co4	1750	20	30	2.35	1.57	98.3 (96%)	2.2 (4%)	101.5	5.6	135.7
9	Co4	1750	40	30	4.05	2.70	52.5 (88%)	2.7 (12%)	78.3	15.0	131.2
10	Co4	1750	50	30	4.80	3.20	48.6 (72%)	2.5 (28%)	74.7	20.2	131.4
11	Co4	1750	60	30	4.00	2.67	62.4 (63%)	1.5 (37%)	71.3	21.1	130.6
12	Co4	1750	80	30	3.40	2.26	42.1 (45%)	1.4 (55%)	69.5	22.7	130.6

13	Co4	1750	50	5	1.65	6.60	35.6 (22%)	1.6 (78%)	52.4	23.8	128.6
14	Co4	1750	50	15	3.42	4.56	51.2 (36%)	42.8 (64%)	59.9	22.3	130.5
15	Co4	1750	50	45	4.95	2.20	64.4 (62%)	2.6 (38%)	79.6	22.9	131.6
16	Co4	1750	50	60	5.15	1.72	72.3 (70%)	21.3 (30%)	90.8	22.3	131.9
17 ^e	Co4	1750	50	30	2.90	1.90	34.2 (76%)	1.3 (24%)	53.0	13.0	131.0
18 ^f	Co4	1750	50	30	0.10	0.07	19.5 (82%)	3.5 (18%)	39.6	10.1	126.3
19	Co1	1750	50	30	5.43	3.62	52.2 (64%)	1.2 (36%)	69.8	20.1	130.5
20	Co2	1750	50	30	4.75	3.16	69.1 (70%)	2.4 (30%)	108.8	22.1	132.1
21	Co3	1750	50	30	2.12	1.41	90.2 (89%)	2.7 (11%)	124.5	19.4	133.5
22	Co5	1750	50	30	3.73	2.48	85.3 (71%)	2.5 (29%)	112.3	22.9	133.3

^a Conditions: 3.0 μmol of **Co4**; 100 mL toluene, 10 atm ethylene. 30 min, ^b Values in units of $10^6 \text{ g(PE) mol}^{-1} (\text{Co}) \text{ h}^{-1}$. ^c Determined by GPC, M_p and M_w : kg mol^{-1} . ^d Determined by DSC. ^e 5 atm ethylene. ^f 1 atm ethylene.

With the Al/Co molar ratio fixed at 1750, **Co4**/MMAO was screened at temperatures between 20 and 60 °C and additionally at 80 °C (entries 4 and 8 – 12, Table 3). The highest activity of $3.20 \times 10^6 \text{ g PE mol}^{-1} (\text{Co}) \text{ h}^{-1}$ was achieved at 50 °C (entry 10, Table 3) above which the performance gradually dropped off. Nonetheless, even at 80 °C, the activity still remained higher (up to $2.26 \times 10^6 \text{ g PE mol}^{-1} (\text{Co}) \text{ h}^{-1}$) than that observed by the **F**-type cobalt counterparts (Chart 1).^{12c} The molecular weight of the polymers was found to decrease from 101.5 to 69.5 kg mol^{-1} on raising the temperature which was accompanied by a broadening in the molecular weight distribution (5.6 to 22.7) (entries 4 and 8 – 12, Table 3). Indeed, the presence of two M_p peaks (peak 1 and peak 2) in their GPC curves (Fig. 7) supports a bimodal distribution for the polymers across the entire

temperature range with the lower molecular weight fraction becoming the major component at higher temperature (Fig. 7); an observation attributable to the difference in rates of chain termination of the two likely competing processes.

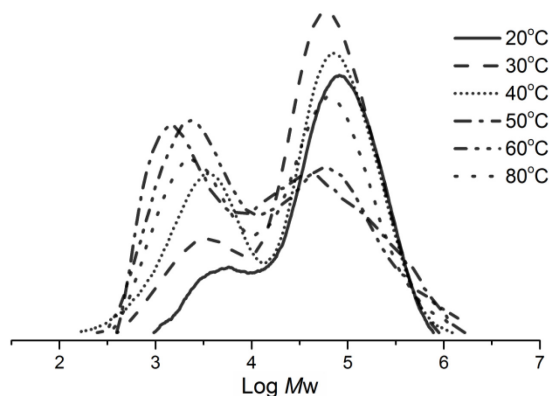


Fig. 7. GPC curves for the polyethylenes obtained using **Co4/MMAO** at different reaction temperatures (10 atm of ethylene, Al/Co ratio = 1750 and 30 minute run time)

To explore the lifetime of the active species derived from **Co4/MMAO**, the polymerization runs were conducted over 5, 15, 30, 45 and 60 minutes (entries 10 and 13 – 16, Table 3) with the Al/Co ratio at 1750 and the temperature at 50 °C. The highest activity of 6.60×10^6 g PE mol⁻¹ (Co) h⁻¹ was observed after 5 minutes (entry 13, Table 3). Indeed, the activity was more than twice that observed after 30 minutes (entry 4, Table 3), which highlights both the rate at which the active species was generated after MMAO addition and also the onset of catalyst deactivation over time.^{14a,19} Meanwhile, the activity gradually decreased as the run time was increased from 5 to 60 minutes; this behavior is consistent with previous reports.^{4a,b,14a} Again two M_p peaks (peak 1 and peak 2) in the GPC curves (Fig. 8) were apparent consistent with bimodal distributions for all the

polymers with the higher molecular weight fraction becoming the major component with more extended run times (Fig. 8). To examine any potential induction period for the polymerization, a 1 minute run was additionally performed (See SI). Indeed this run displayed the highest activity (8.2×10^6 g PE mol⁻¹ (Co) h⁻¹), a finding that is consistent with no induction period. With regard to the ethylene pressure, the activity was found to drop by more than a half when lowered from 10 to 5 atmospheres (entries 17 vs. 7, Table 3); at 1 atmosphere only trace amounts of polymer could be detected (entry 18, Table 3).

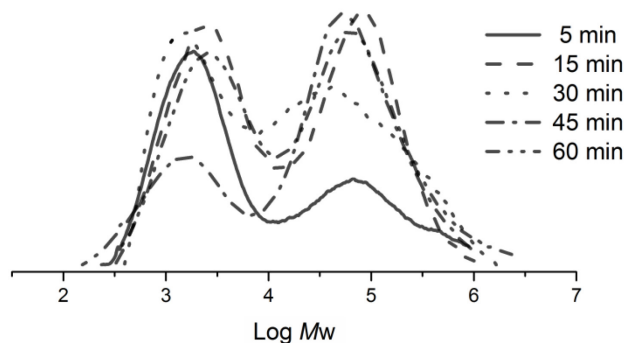


Fig. 8. GPC curves for the polyethylenes obtained using **Co4**/MMAO at different reaction times (10 atm of ethylene, Al/Co ratio = 1750 and at 50 °C)

Using the optimized conditions established for **Co4**/MMAO (*i.e.*, Al/Co ratio of 1750, run temperature = 50 °C), **Co1** – **Co3** and **Co5** were additionally screened for ethylene polymerization. All these MMAO-promoted systems showed high activities (entries 10 and 19 – 22, Table 3) and indeed generally higher values ($1.41 - 3.62 \times 10^6$ g PE mol⁻¹ (Co) h⁻¹) than that observed with MAO as co-catalyst ($0.57 - 2.89 \times 10^6$ g PE mol⁻¹ (Co) h⁻¹) (entries 3 and 18 – 21, Table 2). In terms of their relative catalytic performance the

activities were found to fall in the order **Co1** (2,6-dimethyl) > **Co4** (2,4,6-trimethyl) > **Co2** (2,6-diethyl) > **Co5** (2,6-diethyl-4-methyl) > **Co3** (2,6-diisopropyl), which reveals some differences to that seen with MAO. In particular, the *para*-methyl-containing pre-catalysts **Co4** and **Co5** are now less active than their proton-containing counterparts, **Co1** and **Co2**, suggesting a negative effect of the electron donating methyl group and no beneficial solubility effects on the activity.^{3h,10a,12a,13,22} Otherwise, similar steric factors are at play with increased hindrance of the N-aryl group substituents leading to less active catalysts. As with the MAO study, the most hindered pre-catalyst **Co3** (2,6-diisopropyl) displayed the lowest activity but produced polyethylene with the highest molecular weight (entry 21, Table 3); similar findings have been reported for cobalt-containing **C**, **D** and **F** (Chart 1).^{12,13} The melt temperatures of all the polymers were found to fall in the range 126.5 – 135.7 °C, values quite typical of highly linear polyethylenes. On comparison of the DSC curves of the polymers obtained using MAO, the melting endotherms of MMAO-derived polymers exhibit, in most cases, slightly broader endotherms (Fig S42 – S49); an observation that is consistent with these polymers displaying broader molecular weight distributions. Further support for the linearity of the materials was provided by the high temperature ¹³C NMR data for the polymer obtained using **Co4**/MMAO (entry 10, Table 3), in which a high intensity singlet at δ 29.96 supports the presence of equivalent $-(CH_2)_n-$ repeat units (Fig. S11).¹⁰⁻¹⁴ Interestingly, lower intensity peaks at δ 32.22, 22.92 and 14.24 corresponding to *n*-propyl end-groups are also detectable (peaks 1 - 3 in insert to Fig. 10).³ⁿ By contrast, there is no evidence for

peaks corresponding to iso-butyl end-groups, precluding chain transfer to $\text{Al}(i\text{-Bu})_3$ and its derivatives present in MMAO.³ⁿ Furthermore, no peaks attributable to unsaturated chain ends could be identified which may suggest the absence of termination via β -H elimination. Therefore, it would appear that the bimodal polymer generated using **Co4**/MMAO (entry 10, Table 3) contains substantial amounts of saturated chain ends formed through transfer to selectively AlMe_3 and its derivatives present in MMAO.^{2b,c}

To further probe the chain-end types, we also recorded the ^{13}C NMR spectra of polymers obtained at 1000 (entry 1, Table 3) and 3000 (entry 7, Table 3) equivalents of MMAO (with **Co4** a pre-catalyst) in which distinct mono- and bimodal behavior had been observed, respectively (Fig. S12). Examination of the spectrum of the bimodal polymer (3000 equivalents) showed the $-(\text{CH}_2)_n-$ repeat unit as a singlet at δ 29.96 flanked by lower intensity peaks at 32.22, 22.92 and 14.24 corresponding to n-propyl end-groups (peaks 1 – 3 in Fig. S12) as seen earlier. Unfortunately, the spectrum of the higher molecular weight monomodal polymer (1000 equivalents) revealed only a peak for the $-(\text{CH}_2)_n-$ repeat unit and no reliable information regarding the chain end types (Fig. S12).¹⁰⁻¹⁴

CONCLUSIONS

A one-pot template approach has been successfully employed to generate the cobalt(II) chloride chelates, **Co1** – **Co5**, each bearing the ring-fused α,α' -bis(arylimino)-2,3:5,6-bis(hexamethylene)pyridine ligand that differs in the substitution pattern of the N-aryl

group. On activation with MMAO or MAO, all the pre-catalysts exhibited high activity towards ethylene polymerization and produced highly linear polyethylenes. The **Co1** – **Co5**/MAO systems generally gave higher molecular weights than their **Co1** – **Co5**/MMAO counterparts. By contrast, the **Co1** – **Co5**/MMAO systems generally exhibited better activities than with **Co1** – **Co5**/MAO, but displayed broader and in many cases bimodal distributions. In terms of the steric and electronic properties of the pre-catalysts, the complexes containing less bulky N-aryl groups favored higher activities while the bulkier derivatives gave higher molecular weights. Unexpectedly, the presence of a *para*-methyl groups in **Co4** and **Co5** has a positive effect of on the catalytic activity with MAO but negative effect with MMAO.

EXPERIMENTAL SECTION

General Considerations: All manipulations involving air- and moisture-sensitive compounds were carried out under nitrogen atmosphere using standard Schlenk techniques. Toluene was heated to reflux over sodium and distilled under nitrogen prior to use. MAO (1.46 M solution in toluene) and MMAO (1.93 M in *n*-heptane) were purchased from Akzo Nobel Corp. High-purity ethylene was purchased from Beijing Yansan Petrochemical Co. and used as received. Other reagents were purchased from Aldrich, Acros or local suppliers. NMR spectra were recorded with a Bruker DMX 500, and 600 MHz instrument at ambient temperature using TMS as internal standard. The magnetic susceptibility measurements were recorded according to the NMR method

described by Evans.^{3b,17} IR spectra were recorded with a PerkinElmer System 2000 FTIR spectrometer. Elemental analysis was carried out with a Flash EA 1112 microanalyzer. Molecular weights and molecular weight distributions of the polymers were determined with an Agilent PLGPC 220 GPC system at 150 °C, with 1,2,4-trichlorobenzene as solvent. The melting points of the polyethylenes were measured from the fourth scanning run on a PerkinElmer TA-Q2000 differential scanning calorimeter under a nitrogen atmosphere. A sample of about 5.0 mg was heated to 160 °C at a rate of 20 °C min⁻¹, maintained for 2 min at 160 °C to remove the thermal history and then cooled to - 40 °C at a rate of 20 °C min⁻¹. ¹³C NMR spectra of the polyethylenes were recorded with a Bruker DMX 300 MHz instrument at 135 °C in 1,1,2,2-[D₂]-tetrachloroethane with TMS as internal standard.

Preparation of 2,3:5,6-bis(hexamethylene)pyridine

Based on a literature procedure,^{16a} a mixture of cyclooctanone (252.0 g, 2.00 mol), morpholine (348.0 g, 4.00 mol) and *p*-toluenesulfonic acid (25.0 g) in freshly distilled toluene (750 mL) was placed in a 2 L round-bottom flask fitted with a Dean-Stark water separator and stirred at reflux for 60 h. After removal of a pre-determined amount of water (~ 36 mL H₂O), the reaction was stopped and the solvent removed under reduced pressure to give a thick solid mass (400 g). This crude product was then combined with paraformaldehyde (37.5 g, 0.42 mol) in 1,4-dioxane (600 mL) and stirred at reflux for 12 h in a 2 L round-bottom flask. On cooling to room temperature the reaction mixture was

cooled and acidified with 5 N HCl, the aqueous layer extracted with CH₂Cl₂ (3 × 300 mL) and the combined organic layers washed with water (2 × 100 mL) and dried over anhydrous Na₂SO₄. Following solvent evaporation, the residue was distilled [~10 mmHg, 98 °C] to give the crude product (360 g). This material was then treated with NH₄OAc (210.0 g, 2.77 mol) in AcOH (500 mL) and stirred at reflux for 18 h in a 2 L round-bottom flask. The solution was cooled, made basic with a 50% aqueous NaOH solution and then extracted with CH₂Cl₂ (3 × 400 mL). The combined organic layers were washed with water (2 × 100 mL) and dried over anhydrous MgSO₄. Evaporation of the solvent gave 250 g of a dark oil which was treated with acetone (600 mL) and the mixture stirred at 0 °C for 30 min to give a white precipitate. The precipitate was filtered affording 2,3:5,6-bis(hexamethylene)pyridine as a white solid (63.3 g, 26%). Mp: 108-109 °C. The chemical shifts of all the signals in the NMR spectra are consistent with those reported by Thummel and Jahng.^{16a} ¹H NMR (500 MHz, CDCl₃, TMS): 7.07 (s, 1H, Ar-H), 2.92 (dd, 4 H, *J* = 5.3, 6.6 Hz, Ar CH, Py-CH₂ × 2), 2.70 (dd, 4 H, *J* = 5.1, 6.6 Hz, Ar-CH₂ × 2), 1.86 – 1.54 (m, 8H, PyCH₂-CH₂ × 2 and ArCH₂-CH₂ × 2), 1.42 – 1.24 (m, 8H, CH₂ × 4). ¹³C {¹H} NMR (125 MHz, CDCl₃, TMS) δ 157.88, 137.29, 133.59, 34.06, 32.29, 31.47, 30.84, 26.06, 25.96. Anal. Calcd for C₁₇H₂₅N (243.20): C, 83.89, H, 10.35, N, 5.75%; found C, 83.86, H 10.36, N 5.74%.

Preparation of α,α' -dioxo-2,3:5,6-bis(hexamethylene)pyridine

Based on a literature procedure,^{16a} a mixture of 2,3:5,6-bis(hexamethylene)pyridine

(24.30 g, 0.10 mol), benzaldehyde (106.00 g, 1.00 mol) and acetic anhydride (81.60 g, 0.80 mol) was heated at 180 °C for 72 h under an atmosphere of nitrogen. The mixture was then cooled to room temperature and the solvent evaporated under reduced pressure to give a residue that was dissolved in dry CH₂Cl₂ (500 mL). The resulting solution was cooled to -40 °C using a low temperature cold trap and ozone/oxygen bubbled through the solution for 3 h until a light yellow color remained. The ozone addition was ceased and oxygen alone was bubbled through the solution for a further 10 min. so as to purge out the remaining ozone. Me₂S (10 mL) was added and mixture then warmed to room temperature and stirred for 2 h. The solution was concentrated under reduced pressure and the residue diluted with CH₂Cl₂ (250 mL), washed with water (2 × 50 mL) and dried over anhydrous MgSO₄. Following filtration the mixture was evaporated under reduced pressure to give a solid residue which was purified by chromatography on silica gel with petroleum ether/ethyl acetate (v:v = 1:1) as eluent. The title compound was obtained as a light yellow powder (6.77 g, 25%). Mp: 103 – 104 °C. The chemical shifts of all the signals in the NMR spectra are consistent with those reported by Thummel and Jahng.^{16a}

¹H NMR (500 MHz, CDCl₃, TMS) δ 7.32 (s, 1H, Ar-H), 2.83 – 2.75 (m, 8H, Ar-CH₂ × 2 and CO-CH₂ × 2), 1.76 (tt, *J* = 12.4, 6.5 Hz, 8H, ArCH₂-CH₂ × 2 and COCH₂-CH₂ × 2), 1.63 – 1.58 (m, 4H, CH₂ × 2). ¹³C {¹H} NMR (125 MHz, CDCl₃, TMS) δ 208.84 (C=O), 154.89, 138.99, 134.36, 44.90, 31.01, 28.32, 27.07, 23.23. Anal. Calcd for C₁₇H₂₁NO₂ (271.35): C, 75.24, H, 7.80, N, 5.16%; found C 75.12, H 7.70, N 5.09%.

Preparation of [2,3:5,6-{C₅H₁₀C(NAr)}₂C₅HN]CoCl₂

(a) Ar = 2,6-Me₂C₆H₃ (**Co1**). A suspension of α,α' -dioxo-2,3:5,6-bis(hexamethylene)pyridine (0.27 g, 1.0 mmol), 2,6-dimethylaniline (0.49 g, 4.0 mmol) and CoCl₂·6H₂O (0.24 g, 0.90 mol) in glacial acetic acid (15 mL) was stirred and heated to reflux for 12 h. On cooling to room temperature, an excess of diethyl ether was added to precipitate the crude product which was collected before being re-dissolved in methanol (5 mL). The methanol solution was concentrated and the product again precipitated with diethyl ether. Following filtration and drying under reduced pressure **Co1** was obtained as a brown powder (0.50 g, 92%). ¹H NMR (600 MHz, CDCl₃) δ 42.16 (1H, Py-*H_p*), 15.49 (4H, N=CCH₂), 13.20 (4H, Ar-*H_m*), 2.50 – 0.33 (16H, CH₂), -7.36 (2H, Ar-*H_p*), -16.43 (12H, Ar_o-CH₃). FT-IR (cm⁻¹): 2965 (w), 2926 (m), 2859 (w), 1646 (w), 1598 ($\nu_{C=N}$, m), 1542 (w), 1447 (s), 1378 (w), 1345 (w), 1253 (s), 1227 (w), 1202 (w), 1156 (w), 1117 (w), 1073 (w), 1034 (w), 921 (w), 889 (w), 768 (s). Anal. Calcd for C₃₃H₃₉Cl₂N₃Co (607.52): C, 65.24, H, 6.47, N, 6.91%; found C 65.14, H, 6.42, N, 6.82%. μ_{eff} (Evans' NMR method) = 3.9 μ_B .

(b) Ar = 2,6-Et₂C₆H₃ (**Co2**). Using a one-pot procedure similar to that described for **Co1**, **Co2** was obtained as a brown powder (0.54 g, 90%). ¹H NMR (600 MHz, CDCl₃) δ 42.26 (1H, Py-*H_p*), 15.25 (4H, N=CCH₂), 14.03 (4H, Ar-*H_m*), 3.14 – 0.76 (16H, CH₂), -7.09 (2H, Ar-*H_p*), -10.63 (4H, CH₂Me), -14.18 (12H, CH₃). FT-IR (cm⁻¹): 2964 (w), 2928 (m), 2860 (w), 1653 (w), 1596 ($\nu_{C=N}$, m), 1540 (w), 1456 (s), 1377 (w), 1347 (w), 1252 (s), 1226 (w), 1199 (w), 1155 (w), 1117 (w), 1066 (w), 1034 (w), 935 (w), 887 (w), 790 (s),

755 (s). Anal. Calcd for $C_{37}H_{47}Cl_2N_3Co$ (663.63): C, 66.96, H, 7.14, N, 6.33%; found C 66.84, H 6.97, N 6.13%. μ_{eff} (Evans' NMR method) = 4.1 μ_B

(c) Ar = 2,6-*i*-Pr₂C₆H₃ (**Co3**). Using a one-pot procedure similar to that described for **Co1**, **Co3** was obtained as a brown powder (0.58 g, 89%). ¹H NMR (600 MHz, CDCl₃) δ 41.48 (1H, Py-*H*_p), 14.13 (8H, N=CCH₂ and Ar-*H*_m), 4.59 – 0.19 (32H, CH₂ and CH₃), -5.94 (2H, Ar-*H*_p), -14.03 (8H, CH₂Me and CH₃). FT-IR (cm⁻¹): 2961 (w), 2927 (m), 2864 (w), 1646 (w), 1597 ($\nu_{C=N}$, m), 1558 (w), 1540 (w), 1457 (s), 1386 (w), 1362 (w), 1327 (w), 1250 (s), 1226 (w), 1194 (w), 1154 (w), 1105 (w), 1057 (w), 1005 (w), 942 (w), 892 (w), 790 (m), 779 (w), 754 (s). Anal. Calcd for $C_{41}H_{55}Cl_2N_3Co$ (719.73): C, 68.42, H, 7.70, N, 5.84%; found: C, 68.22, H, 7.53, N, 5.74%. μ_{eff} (Evans' NMR method) = 4.0 μ_B

(d) Ar = 2,4,6-Me₃C₆H₂ (**Co4**). Using a one-pot procedure similar to that described for **Co1**, **Co4** was obtained as a brown powder (0.51 g, 89%). ¹H NMR (600 MHz, CDCl₃) δ 41.49 (1H, Py-*H*_p), 15.36 (4H, N=CCH₂), 12.83 (4H, Ar-*H*_m), 3.78 – 0.83 (16H, CH₂), -4.84 (6H, Ar_p-CH₃), -15.05 (12H, Ar_o-CH₃). FT-IR (cm⁻¹): 2926 (m), 2860 (w), 1653 (w), 1596 ($\nu_{C=N}$, m), 1558 (w), 1540 (w), 1476 (s), 1447 (s), 1346 (w), 1306 (w), 1251 (m), 1228 (s), 1212 (w), 1179 (w), 1133 (w), 1072 (w), 1034 (w), 936 (w), 887 (w), 853 (s), 795 (w), 735 (m). Anal. Calcd for $C_{35}H_{43}Cl_2N_3Co$ (635.57): C, 66.14, H, 6.82, N, 6.61% found: C, 66.02, H, 6.62, N, 6.52%. μ_{eff} (Evans' NMR method) = 4.0 μ_B

(e) Ar = 2,6-Et₂-4-MeC₆H₂ (**Co5**). Using a one-pot procedure similar to that described for **Co1**, **Co5** was obtained as a brown powder (0.56 g, 90%). ¹H NMR (600 MHz, CDCl₃) δ 42.25 (1H, Py-*H*_p), 15.25 (4H, N=CCH₂), 14.04 (4H, Ar-*H*_m), 4.64 – 0.68 (16H, CH₂),

-7.07 (6H, Ar_p-CH₃), -10.62 (8H, CH₂Me), -14.15 (12H, Ar_o-CH₃). FT-IR (cm⁻¹): 2965 (w), 2929 (m), 2862 (w), 1653 (w), 1594 (ν_{C=N}, m), 1541 (w), 1489 (w), 1457 (s), 1375 (w), 1338 (w), 1251 (s), 1227 (w), 1209 (w), 1179 (w), 1157 (w), 1068 (w), 1036 (w), 961 (w), 885 (w), 858 (s), 789 (w), 737 (m). Anal. Calcd for C₃₉H₅₁Cl₂N₃Co (691.68): C, 67.72, H, 7.43 N, 6.08% found: C, 67.55, H, 7.26 N, 5.98%. μ_{eff} (Evans' NMR method) = 4.5 μ_B

Polymerization studies

Ethylene polymerization at 5/10 atm ethylene pressure.

The polymerization at 5 or 10 atm of ethylene pressure was performed in a stainless steel autoclave (250 mL) equipped with an ethylene pressure control system, a mechanical stirrer and a temperature controller. The autoclave was evacuated and refilled with ethylene three times. When the required temperature was reached, the complex (3 μmol) was dissolved in toluene (30 mL) in a Schlenk tube then injected into the autoclave containing ethylene (~ 1 atm), followed by the addition of more toluene (30 mL). The required amount of co-catalyst (MAO and MMAO) and additional toluene were added successively by syringe taking the total volume of toluene to 100 mL. The autoclave was immediately pressurized with 5/10 atm. pressure of ethylene and the stirring commenced. After the required reaction time, the reactor was cooled with a water bath and the excess ethylene was vented. The reaction

quenched with 10% hydrochloric acid in ethanol. The polymer was collected and washed with ethanol and dried under reduced pressure at 50 °C and weighed.

Ethylene polymerization at 1 atm ethylene pressure. The polymerization at 1 atm ethylene pressure was carried out in a Schlenk tube. Under ambient ethylene atmosphere (1 atm), **Co4** (3.0 μmol) was added followed by toluene (30 mL) and then the required amount of co-catalyst (MAO, MMAO) introduced by syringe. The solution was then stirred at the required temperature under ambient ethylene atmosphere (1 atm). After 30 min, the solution was quenched with 10% hydrochloric acid in ethanol. The polymer was washed with ethanol, dried under reduced pressure at 40 °C and then weighed.

X-ray structure determination

Single-crystal X-ray diffraction studies of **Co2** and **Co3** were conducted on a Rigaku Sealed Tube CCD (Saturn 724+) diffractometer with graphite-monochromated Mo-K α radiation ($\lambda = 0.71073 \text{ \AA}$) at 173(2) K and the cell parameters were obtained by global refinement of the positions of all collected reflections. Intensities were corrected for Lorentz and polarization effects and empirical absorption. The structures were solved by direct methods and refined by full-matrix least-squares on F^2 . All non-hydrogen atoms were refined anisotropically and all hydrogen atoms were placed in calculated positions. Structural solution and refinement were performed by using the SHELXTL-97 package.²³

Crystal data and processing parameters for **Co2** and **Co3** are summarized in supporting

information (Table S3).

ASSOCIATED CONTENT

The Supporting Information is available free of charge on the ACS Publications website at DOI:10.1021/om____. X-ray crystallographic data in CIF for CCDC 1584270 (**Co2**) and 1584271 (**Co3**) available free of charge from The Cambridge Crystallographic Data Centre.

AUTHOR INFORMATION

Corresponding Author

*E-mail: whsun@iccas.ac.cn; Tel: +86-10-62557955; Fax: +86-10-62618239 (W.-H.S).

*E-mail: gas8@leicester.ac.uk; Tel: +44-116-2522096 (G.A.S.)

*E-mail: qbinliu@sina.com; Tel: +86-0311-80787432 (Q. L.)

ORCID

Zheng Wang: 0000-0003-0608-8093

Gregory A. Solan: 0000-0002-9833-6666

Qaiser Mahmood: 0000-0002-1808-2492

Qingbin Liu: 0000-0002-7175-0760

Yanping Ma: 0000-0003-3106-9724

Xiang Hao: 0000-0002-4232-5861

Wen-Hua Sun: 0000-0002-6614-9284

Notes

The authors declare no competing financial interest.

ACKNOWLEDGMENTS

This work was supported by the National Natural Science Foundation of China (No. U1362204, 21476060 and 51473170). GAS thanks the Chinese Academy of Sciences for a Visiting Fellowship.

REFERENCES

- (1) (a) Small, B. L.; Brookhart, M. and Bennett, A. M. A. *J. Am. Chem. Soc.*, **1998**, *120*, 4049–4050; (b) Britovsek, G. J. P.; Gibson, V. C.; Kimberley, B. S.; Maddox, P. J.; McTavish, S. J.; Solan, G. A.; White, A. J. P. and Williams, D. J. *Chem. Commun.*, **1998**, 849–850; (c) Britovsek, G. J. P.; Bruce, M.; Gibson, V. C.; Kimberley, B. S.; Maddox, P. J.; Mastroianni, S.; McTavish, S. J.; Redshaw, C.; Solan, G. A.; Stromberg, S.; White, A. J. P. and Williams, D. J. *J. Am. Chem. Soc.*, **1999**, *121*, 8728–8740
- (2) For reviews see (a) Flisak, Z.; Sun, W.-H. *ACS Catal.* **2015**, *5*, 4713-4724; (b)

Gibson, V. C.; Solan, G. A. in *Catalysis without Precious Metals* (Ed. M. Bullock), Wiley-VCH, Weinheim, **2010**, 111-141; (c) Gibson, V. C.; Solan, G. A. *Top. Organomet. Chem.* **2009**, *26*, 107-158; (d) Bianchini, C.; Giambastiani, G.; Luconi, L.; Meli, A. *Coord. Chem. Rev.* **2010**, *254*, 431–455; (e) Gibson, V. C.; Redshaw, C.; Solan, G. A. *Chem. Rev.* **2007**, *107*, 1745-1776; (f) Bianchini, C.; Giambastiani, G.; Rios, I. G.; Mantovani, G.; Meli, A.; Segarra, A. M. *Coord. Chem. Rev.* **2006**, *250*, 1391-1418; (g) Ma, J.; Feng, C.; Wang, S.; Zhao, K. -Q.; Sun, W. -H.; Redshaw, C.; Solan, G. A. *Inorg. Chem. Front.* **2014**, *1*, 14-34; (h) Zhang, W.; Sun, W. -H.; Redshaw, C.; *Dalton Trans.* **2013**, *42*, 8988-8997; (i) Jie, S.; Sun, W.-H.; Xiao, T.; *Chin. J. Polym. Sci.* **2010**, *28*, 299-304; (j) Xiao, T.; Zhang, W.; Lai, J.; Sun, W.-H. *C. R. Chim.* **2011**, *14*, 851- 855; (k) Burcher, B.; Breuil, P. -A. R.; Magna, L. and H. Olivier-Bourbigou, *Top. Organomet. Chem.* **2015**, *50*, 217–258

- (3) (a) Britovsek, G. J. P.; Gibson, V. C.; Kimberley, B. S.; Mastroianni, S.; Redshaw, C.; Solan, G. A.; White, A. J. P.; Williams, D. J. *J. Chem. Soc., Dalton Trans.* **2001**, 1639-1644; (b) Britovsek, G. J. P.; Gibson, V. C.; Spitzmesser, S. K.; Tellmann, K. P.; White, A. J. P.; Williams, D. J.; *J. Chem. Soc., Dalton Trans.* **2002**, 1159–1171; (c) Britovsek, G. J. P.; Gibson, V. C.; Hoarau, O. D.; Spitzmesser, S. K.; White, A. J. P.; Williams, D. J. *Inorg. Chem.* **2003**, *42*, 3454–3465; (d) Kaul, F.; Puchta, K.; Frey, G.; Herdtweck, E.; Herrmann, W. *Organometallics* **2007**, *26*, 988-999; (e) Guo, L.; Gao, H.; Zhang, L.; Zhu, F.; Wu, Q. *Organometallics* **2010**, *29*, 2118–2125; (f) Smit, T. M.; Tomov, A. K.; Britovsek, G. J. P.; Gibson, V. C.; White, A. J. P.; Williams, D. J. *Catal.*

Sci. Technol., **2012**, *2*, 643-655; (g) Yu, J.; Liu, H.; Zhang, W.; Hao, X.; Sun, W.-H. *Chem Comm.*, **2011**, *47*, 3257-3259; (h) Zhao, W.; Yu, J.; Song, S.; Yang, W.; Liu, H.; Hao, X.; Redshaw, C.; Sun, W.-H. *Polymer* **2012**, *53*, 130–137; (i) Cao, X.; He, F.; Zhao, W.; Cai, Z.; Hao, X.; Shiono, T.; Redshaw, C.; Sun, W.-H.; *Polymer* **2012**, *53*, 1870–1880; (j) Sun, W. -H.; Zhao, W.; Yu, J.; Zhang, W.; Hao, X.; Redshaw, C.; *Macromol. Chem. Phys.* **2012**, *213*, 1266-1273; (k) Wang, S.; Li, B.; Liang, T.; Redshaw, C.; Li, Y.; Sun, W.-H. *Dalton Trans.* **2013**, *42*, 9188–9197; (l) Zhang, W.; Wang, S.; Du, S.; Guo, C.-Y.; Hao, X.; Sun, W.-H. *Macromol. Chem. Phys.* **2014**, *215*, 1797–1809; (m) Zhao, W.; Yue, E.; Wang, X.; Yang, W.; Chen, Y.; Hao, X.; Cao, X.; Sun, W.-H. *J. Polym. Sci., Part A: Polym. Chem.*, **2017**, *55*, 988–996; (n) Semikolenova, N. V.; Sun, W. -H.; Soshnikov, I. E.; Matsko, M. A.; Kolesova, O. V.; Zakharov, V. A.; Bryliakov, K. P. *ACS Catal.*, **2017**, *7*, 2868-2877.

(4) (a) Yu, J.; Huang, W.; Wang, L.; Redshaw, C.; Sun, W. -H. *Dalton Trans.* **2011**, *40*, 10209–10214; (b) Lai, J.; Zhao, W.; Yang, W.; Redshaw, C.; Liang, T.; Liu, Y.; Sun, W.-H. *Polym. Chem.* **2012**, *3*, 787 -793; (c) He, F.; Zhao, W.; Cao, X.-P.; Liang, T.; Redshaw, C.; Sun, W.-H. *J. Organomet. Chem.* **2012**, *713*, 209-216; (d) Yue, E.; Zeng, Y.; Zhang, W.; Sun, Y.; Cao, X. -P.; Sun, W.-H.; *Sci. China Chem.* **2016**, *59*, 1291–1300.

(5) (a) Sun, W. -H.; Hao, P.; Zhang, S.; Shi, Q.; Zuo, W.; Tang, X.; Lu, X.; *Organometallics*, **2007**, *26*, 2720–2734; (b) Chen, Y.; Hao, P.; Zuo, W.; Gao, K.; Sun, W.-H. *J. Organomet. Chem.*, **2008**, *693*, 1829–1840; (c) Xiao, L.; Gao, R.; Zhang, M.;

- Li, Y.; Cao, X.; Sun, W.-H.; *Organometallics*, **2009**, *28*, 2225–2233; (d) Gao, R.; Li, Y.; Wang, F.; Sun, W.-H.; Bochmann, M. *Eur. J. Inorg. Chem.*, **2009**, 4149–4156.
- (6) Wang, K.; Wedeking, K.; Zuo, W.; Zhang, D.; Sun, W. -H. *J. Organomet. Chem.*, **2008**, *693*, 1073–1080.
- (7) Zhang, S.; Sun, W.-H.; Xiao, T.; Hao, X. *Organometallics*, **2010**, *29*, 1168–1173.
- (8) (a) Wang, L.; Sun, W.-H.; Han, L.; Yang, H.; Hu, Y.; Jin, X. *J. Organomet. Chem.*, **2002**, *658*, 62–70; (b) Pelletier, J. D. A.; Champouret, Y. D. M.; Cardoso, J.; Clowes, L.; Gañete, M.; Singh, K.; Thanarajasingham, V.; Solan, G. A. *J. Organomet. Chem.*, **2006**, *691*, 4114-4123; (c) Jie, S.; Zhang, S.; Wedeking, K.; Zhang, W.; Ma, H.; Lu, X.; Deng, Y.; Sun, W.-H.; *C. R. Chim.*, **2006**, *9*, 1500–1509; (d) Jie, S.; Zhang, S.; Sun, W. -H.; Kuang, X.; Liu, T.; Guo, J. *J. Mol. Catal. A: Chem.*, **2007**, *269*, 85–96; (e) Jie, S.; Zhang, S.; Sun, W.-H. *Eur. J. Inorg. Chem.*, **2007**, *35*, 5584–5598; (f) Hao, P.; Zuo, W.; Jie, S.; Sun, W.-H. *J. Organomet. Chem.*, **2008**, *693*, 483-491; (g) Zhang, M.; Gao, R.; Hao, X.; Sun, W.-H. *J. Organomet. Chem.*, **2008**, *693*, 3867-3877.
- (9) Sun, W.-H.; Jie, S.; Zhang, S.; Zhang, W.; Song, Y.; Ma, H. *Organometallics*, **2006**, *25*, 666–677.
- (10)(a) Zhang, W.; Chai, W.; Sun, W.-H.; Hu, X.; Redshaw, C.; Hao, X. *Organometallics*, **2012**, *31*, 5039–5048; (b) Sun, W.-H.; Kong, S.; Chai, W.; Shiono, T.; Redshaw, C.; Hu, X.; Guo, C.; Hao, X. *Appl. Catal., A*, **2012**, *447–448*, 67–73.
- (11)(a) Ba, J.; Du, S.; Yue, E.; Hu, X.; Flisak, Z.; Sun, W.-H. *RSC Adv.*, **2015**, *5*,

- 32720–32729. (b) Zhang, Y.; Huang, C.; Hao, X.; Hu, X.; Sun, W.-H. *RSC Adv.*, **2016**, *6*, 91401–91408.
- (12)(a) Huang, F.; Xing, Q.; Liang, T.; Flisak, Z.; Ye, B.; Hu, X.; Yang, W.; Sun, W.-H. *Dalton Trans.*, **2014**, *43*, 16818–16829; (b) Huang, F.; Zhang, W.; Yue, E.; Liang, T.; Hu, X.; Sun, W.-H.; *Dalton Trans.*, **2016**, *45*, 657–666. (c) Huang, F.; Zhang, W.; Sun, Y.; Hu, X.; Solan, G. A.; Sun, W. H. *New J. Chem.* **2016**, *40*, 8012–8023; (d) Zhang, Y.; Suo, H.; Huang, F.; Liang, T.; Hu, X.; Sun, W.-H. *J. Polym. Sci. Part A. Polym. Chem.* **2017**, *55*, 830–842.
- (13) Appukuttan, V. K.; Liu, Y.; Son, B. C.; Ha, C.-S.; Suh, H.; Kim, I. *Organometallics*, **2011**, *30*, 2285–2294.
- (14) (a) Du, S.; Zhang, W.; Yue, E.; Huang, F.; Liang, T.; Sun, W.-H.; *Eur. J. Inorg. Chem.*, **2016**, 1748–1755; (b) Du, S.; Wang, X.; Zhang, W.; Flisak, Z.; Sun, Y.; Sun, W.-H. *Polym. Chem.*, **2016**, *7*, 4188–4197; (c) C. Huang, S. Du, G. A. Solan, Y. Sun, W.-H. Sun, *Dalton Trans.*, **2017**, *46*, 6948–6957.
- (15)(a) Zhou, H.; Wang, S.; Huang, H.; Li, Z.; Plummer, C. M.; Wang, S.; Sun, W.-H.; Chen, Y. *Macromolecules*, **2017**, *50*, 3510–3515; (b) Bunescu, A.; Lee, S.; Li, Q.; Hartwig, J. F. *ACS Cent. Sci.* **2017**, *3*, 895–903.
- (16)(a) Thummel, R. P.; Jahng, Y. *J. Org. Chem.* **1985**, *50*, 2407–2412; (b) Thummel, R. P.; Lefoulon, F.; Cantu, D.; Mahadevan, R. *J. Org. Chem.* **1984**, *49*, 2208–2212.
- (17)(a) Evans, D. F. *J. Chem. Soc.* 1959, 2003–2005; (b) Evans, D. F.; Fazakerley, G. V. and Phillips, P. R. *J. Chem. Soc. A*, 1971, 1931–1934.

- (18)(a) J. Jones, D.; Gibson, V. C.; Green, S. M.; Maddox, P. J.; White, A. J. P.; Williams, D. J. *J. Am. Chem. Soc.* **2005**, *127*, 11037–11046; (b) Tomov, A. K.; Gibson, V. C.; Britovsek, G. J. P.; Long, R. J.; Meurs, M.; Jones, D. J.; Tellmann, K. P.; Chirinos, J. J. *Organometallics* **2009**, *28*, 7033 – 7040.
- (19)Xiao, T.; Hao, P.; Kehr, G.; Hao, X.; Erker, G.; Sun, W.-H. *Organometallics* **2011**, *30*, 4847 – 4853.
- (20)(a) Abu-Surrah, A. S.; Lappalainen, K.; Piironen, U.; Lehmus, P.; Repo, T.; Leskela, M. *J. Organomet. Chem.* **2002**, *648*, 55–61; (b) Sun, W.-H.; Tang, X.; Gao, T.; Wu, B.; Zhang, W.; Ma, H. *Organometallics*, **2004**, *23*, 5037–5047.
- (21)Xing, Q.; Zhao, T.; Du, S.; Yang, W.; Liang, T.; Redshaw, C.; Sun, W.-H. *Organometallics*, **2014**, *33*, 1382-1388.
- (22)(a) Guo, D.; Yang, X.; Yang, L.; Li, Y.; Liu, T.; Hong, H.; Hu, Y. *J. Polym. Sci., Part A: Polym. Chem.*, **2000**, *38*, 2232 - 2238; (b) Guo, D.; Yang, X.; Liu, T.; Hu, Y. *Macromol. Theory Simul.*, **2001**, *10*, 75-78; (c) Guo, D.; Han, L.; Zhang, T.; Sun, W.-H.; Li, T.; Yang, X. *Macromol. Theory Simul.*, **2002**, *11*, 1006-1012.
- (23)Sheldrick, G. M. SHELXTL-97, Program for the Refinement of Crystal Structures. University of Göttingen: Germany, **1997**.

For the Table of Contents use only

Bis(imino)pyridines incorporating doubly fused 8-membered rings as conformationally flexible supports for cobalt ethylene polymerization catalysts

Zheng Wang,^{†,‡} Gregory A. Solan,^{†,#,*} Qaiser Mahmood,^{†,‡} Qingbin Liu,^{§,*} Xiang Hao,[†]

and Wen-Hua Sun^{†,‡,*}

